Polymer Chemistry

Synthesis and Self-Assembly of the Amphiphilic Homopolymers Poly(4-hydroxystyrene) and Poly(4-(4-bromophenyloxy)styrene)

Journal:	*Polymer Chemistry*
Manuscript ID	PY-ART-10-2023-001124.R2
Article Type:	Paper
Date Submitted by the Author:	02-Jan-2024
Complete List of Authors:	Hurley, Christopher; University of Tennessee, Department of Chemistry Changez, Mohammad; University of Buraimi, COHS Johnstone, Megan; University of Tennessee Knoxville College of Engineering, Department of Nutrition Donohoe, Dallas; The University of Tennessee-Knoxville, Nutrition Anwar, Mohammad; AIIMS Alrahbi, Hilal; University of Buraimi, College of Health Sciences; Mays, Jimmy; University of Tennessee, Chemistry Kang, Nam-Goo; University of Tennessee Knoxville College of Engineering, Department of Chemistry

Polymer Chemistry

Paper

Synthesis and Self-Assembly of the Amphiphilic Homopolymers Poly(4-hydroxystyrene) and Poly(4-(4-bromophenyloxy)styrene)

Received 00th January 20xx,
Accepted 00th January 20xx

DOI: 10.1039/x0xx00000x

www.rsc.org/

Christopher M. Hurley[a], Mohammad Changez[b]*, Megan E. Johnstone[c], Hilal Alrahbi[b], Mohammad Faiyaz Anwar[d], Dallas Donohoe[c], Nam-Goo Kang[a]*, Jimmy Mays[a]

Poly(4-(1-ethoxyethoxy)styrene) was synthesized by living anionic polymerization under high vacuum conditions. Amphiphilic derivatives, poly(4-hydroxystyrene) (PHS) and poly(4-(4-bromophenyloxy)styrene) (PBPOS) were synthesized by post-polymerization reactions of poly(4-(1-ethoxyethoxy)styrene). For comparison of hydrogen bonding and halogen bonding, the self-assembly behaviors of both homopolymers, PHS and PBPOS, were evaluated by dynamic/static light scattering (DLS/SLS) in a mixed solvent of water: tetrahydrofuran and water: methanol, respectively. The morphologies of aggregates were recorded using atomic force microscopy (AFM), scanning electron microscope (SEM), and transmission electron microscopy (TEM). PHS forms the hollow micelles in the water: THF mixed solvent and the vesicles in the water: methanol mixed solvent. Also, PBPOS forms the open-mouth vesicles in the water: methanol mixed solvent. PHS vesicles show potential as a template for forming gold nanoparticles and can act as a reservoir of the anti-cancer drug doxorubicin. The release of doxorubicin from PHS vesicles depends on the pH of the release media. The rate of drug release is higher at basic pH. The viability of the colon cancer cell line HCT-116 decreased by 27% compared to an untreated cell line when treated with doxorubicin loaded PHS vesicles.

1. Introduction

The self-assembly of amphiphilic homopolymers has emerged as a growing field of interest within polymer chemistry. The self-assembly behavior of block copolymers is well known, as amphiphilic block copolymers have been shown to form a variety of nanostructures including micelles, vesicles, cylinders, and several other complex structures. The impetus for the self-assembly of block copolymers is the chemical incompatibility of one block in the chosen solvent, and typically combinations of hydrophobic and hydrophilic blocks are used. By careful manipulation of parameters such as the solvent composition, block length, block ratio, and hydrophilic-hydrophobic balance of the block segments used, the nanostructures of the block copolymer self-assembled structures can be tailored.[1-3] Interest in these materials has been spurred on by their applications in a wide variety of fields, including drug delivery, sensing, and nanotechnology.[4-6]

The recent development of polymer-based nano-aggregates by designed homopolymers having a hydrophilic and hydrophobic moiety on either side of the hydrophobic backbone is gaining attention for nanotechnology applications.[7-12] This clever design allows for the formation of homopolymer nano-aggregates in both aqueous and hydrophobic solutions. Furthermore, Lee et al. demonstrate the amphiphilic behavior of poly(2-(4-vinylphenyl)pyridine) in which inter-competition between the hydrophobic polymer backbone and more hydrophilic pendent group in comparison to the backbone allows for the formation of vesicles and micelles in the presence of selective solvent compositions. The resultant nano-aggregates show responsive behavior in response to the surrounding environment.[13,14] Thayamanavan et al. further demonstrated the potential of amphiphilic homopolymers by performing a rearrangement reaction using the core of the micelle as a nanoreactor. When compared to micelles formed from commonly used small molecules and block copolymers, those micelles constructed of homopolymers were more rigid, stable, and confined.[13-17]

Since the discovery of homopolymer self-assembly behavior, two techniques have been developed to synthesize these macromolecules: the "monomer-induced" method and the "hydrophobic-group-induced" method.[1] The "monomer-induced" method relies upon specially designed monomers, with hydrophobic and hydrophilic moieties or hydrophobic polymer backbones with hydrophilic pendent groups, to cause self-assembly.[13,14,18,19] The “hydrophobic-group-induced” method relies upon a hydrophilic homopolymer attached to a large hydrophobic end group to cause self-assembly.[20-25] Amphiphilic homopolymer self-assembly is achieved through intramolecular phase separation and non-covalent intra and intermolecular interactions.[1-3]

[a] Department of Chemistry, University of Tennessee, Knoxville, TN 37996, USA, email: papyrus92@gmail.com
[b] College of Health Sciences, University of Buraimi, Buraimi, Oman, email: mchangez@uob.edu.om
[c] Department of Nutrition, University of Tennessee, Knoxville, TN 37996, USA
[d] Department of Pathology, All Indian Institute of Medical Sciences, Ansari Nager, New Delhi, India
*Corresponding authors
Electronic Supplementary Information (ESI) available: [details of any supplementary information available should be included here]. See DOI: 10.1039/x0xx00000x

Poly(4-hydroxstyrene) (PHS) represents an ideal candidate for amphiphilic homopolymer self-assembly. The rigid and polar nature of the pendent group and the flexible and non-polar polymer backbone are analogous to the poly(2-(4-vinylphenyl(pyridine)) used by Lee et al.[13-15] The recent introduction of acetal functionalized styrene monomers has caused interest in poly(4-hydroxystyrene) to grow.[26-29] Poly(4-hydroxystyrene) has already attracted attention for a variety of applications including photoresist materials, physical gel composites, and pH-responsive materials.[30-32] The direct polymerization of 4-hydroxystyrene by anionic polymerization is not viable due to the acidic nature of the hydroxyl group. Anionic polymerization provides the ability to produce narrow molecular weight distribution polymers with stoichiometric control over the molecular weight.[33] The utilization of protecting groups, to be cleaved after the polymerization to yield poly(4-hydroxystyrene), is the singular successful strategy for anionic polymerization of this monomer. The acetal functionalized monomers represent another element of this same protecting group strategy.[34] The common utilization of acetals as hydroxyl-protecting groups in small molecule chemistry is attributed to their straightforward synthesis and facile deprotection. The mild conditions required to cleave the acetal group from poly(4-(1-ethoxyethoxy)styrene) to produce poly(4-hydroxystyrene) make 4-(1-ethoxyethoxy)styrene an attractive alternative to 4-tert-butoxystyrene, 4-tertbutyl dimethyl siloxy styrene, or 4-acetoxystyrene.

The stability of acetal functionalized polystyrenes to anionic polymerization conditions was demonstrated by Frey et al. when polymerizing in tetrahydrofuran (THF) at a very low temperature (-98 ºC).[26] It was successfully shown that homopolymers of poly(4-(1-ethoxyethoxy)styrene) could be produced with narrow molecular weight distribution over a range of molecular weights (2700-69000 g/mol). Furthermore, they confirmed that the living nature of the chain ends was retained through the synthesis of block copolymers with 2-vinyl pyridine. Hirao et al. first referenced the anionic polymerization of 4-(2-tetrahydropyranyloxy)styrene as well-controlled chain length and narrow dispersity in a footnote as "unpublished research".[35] The report of anionic polymerization of 4-(2-tetrahydropyranyloxy)styrene and the demonstration of its living nature in homo- and block copolymerization was demonstrated by Gopalan et al.[29]

The chemical reactions of the small molecule phenol have been thoroughly reported in the literature and play an important role in the pharmaceutical industry.[13] The potential to adapt known phenol reaction chemistry to yield new polymeric materials by post-polymerization reactions on poly(4-hydroxystyrene) is an area in need of further investigation. The phenol functionality present on each monomer unit potentially allows for the incorporation of previously difficult-to-achieve functionalities. Etherification reactions utilizing the phenol functionality have been used to incorporate many desirable functionalities including electrolytes and macromolecular polymer initiators.[37-41]

Halogen bonding is a non-covalent intra- or inter-molecular force defined by IUPAC in 2013 as a net attractive interaction between an electrophilic region associated with a halogen atom as a Lewis base in a molecular entity and neutral or a nucleophilic region in another, or the same, molecular entity.[42] The potential of halogen bonding is shown by useful applications in the field of synthesis of molecules, cystography, optoelectronics, and biochemistry.[43-45] The halogen bonding in thyroid hormones (THs) are crucial for the endocrine system and play roles in the metabolism of carbohydrate and fat, protein and peptide chemistry, overall growth, and brain development.[46] Although several examples of halogen bonding for polymeric materials have been presented in the literature, the investigation of this molecular force for self-assembly is limited.[6]

In this work, poly(4-(1-ethoxyethoxy)styrene) is produced by anionic polymerization. Post-polymerization reactions yield poly(4-hydroxystyrene) (PHS) and poly(4-(4-bromophenyloxy)styrene) (PBPOS). For understanding the halogen bonding role in the self-assembly of homopolymers in comparison to hydrogen bonding aggregations behavior of PBPOS and PHS homopolymers were investigated by dynamic light scattering (DLS) in aqueous and organic solvent mixtures by atomic force microscopy (AFM), scanning electron microscope (SEM), and transmission electron microscopy (TEM). The capacity of PHS vesicles in solution to transport small molecules and facilitate the formation of gold nanoparticles was also investigated.

2. Experimental

2.1. Materials

4-Bromobenzyl bromide (Sigma Aldrich, 98 %), sodium hydride (Sigma Aldrich, 60% dispersion in mineral oil), concentrated hydrochloric acid (HCl, Fisher Chemical, 36.5 to 38 %), tetrahydrofuran (THF, Sigma Aldrich, anhydrous, >99.9%), methanol (MeOH, Sigma Aldrich, ACS reagent, >99.8 %), 4-(1-ethoxyethoxy)styrene (pEES, Synquest Laboratories), doxorubicin hydrochloride (Thermo Scientific Chemicals), trimethylamine (TEA, Sigma Aldrich, >99.5 %). THF was distilled into the reactor from a purified solvent reservoir on the vacuum manifold.[47] *Sec*-butyllithium was diluted to the desired concentration by hexanes distilled into the appropriate apparatus from a purified solvent reservoir on the vacuum manifold. 4-(1-Ethoxyethoxy)styrene (pEES) was first dried by CaH_2 under a high vacuum before being passed through a glass filter and separated into ampules. The ampules of monomer were then further distilled twice under a dynamic vacuum using moderate heating to assist. Ampules of purified monomer were then diluted to the desired concentration with purified THF. All anionic polymerization reactions were performed under high vacuum in custom-built glass reactors according to standard protocol.[47,48]

2.2. Synthesis

2.2.1. Anionic polymerization of 4-(1-ethoxyethoxy)styrene)

A typical example of the synthesis of poly(4-(1-ethoxyethoxy) styrene) (PpEES) is as follows: the main reactor for polymerization of 4-(1-ethoxyethoxy)styrene was washed with (3-methyl-1,1-diphenylpentyl) lithium solution in hexanes to remove impurities from the reactor. The washing solution was then re-collected by rinsing with distilled hexanes into the purging flask before it was removed from the apparatus. Required volume of *sec*-butyllithium

(0.1 mmol) was introduced by fracturing a break seal and the ampule was rinsed by distilled hexanes to ensure correct stoichiometry. The reactor was then cooled to -98 °C by a liquid N2/methanol bath and 10 mins were allowed for the temperature of the reactor to equilibrate. The ampule of 4-(1-ethoxyethoxy)styrene (Table 1) was cooled to -98 °C before being introduced by fracturing the break seal. The reaction was allowed to proceed for 1.5 hours before being terminated by the introduction of methanol by fracturing a broken seal. The polymer was precipitated into methanol, filtered, re-dissolved in tetrahydrofuran, and rotary evaporated to dryness before being dried in a vacuum oven. (Yield= 93-99%)

2.2.2. Deprotection of poly(4-(1-ethoxyethoxy)styrene)

1.029 g of poly(4-(1-ethoxyethoxy)styrene) was dissolved in 20 ml of THF at room temperature. To the solution, 1 ml of concentrated HCl was added with continuous swirling for 5 minutes. The polymer was then precipitated into deionized water. The precipitated product was then collected by filtration, rinsed with deionized water to remove HCl, and dried in a vacuum oven. (Yield = 78%)

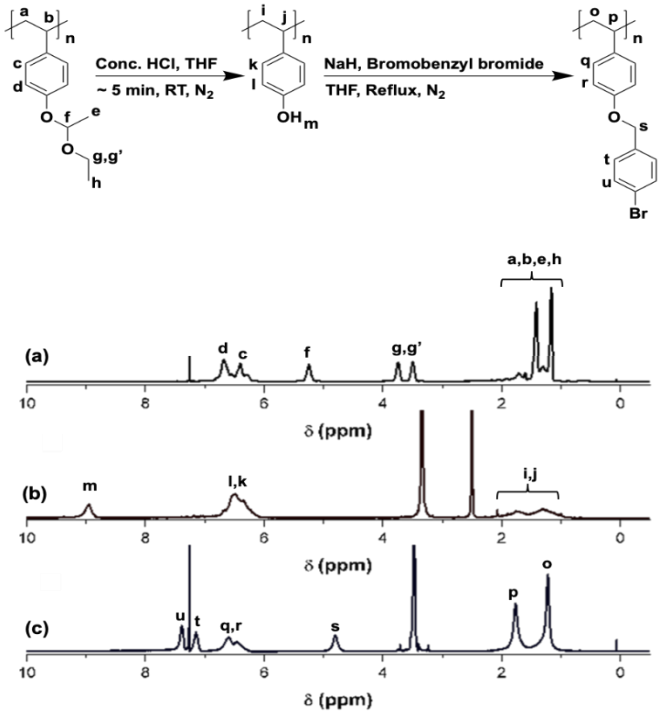

Fig. 1 ^{1}H NMR (500 MHz) spectra of homopolymers (a) poly(4-(1-ethoxyethoxy)styrene) (PpEES) in $CDCl_3$, (b) poly(4-hydroxystyrene) (PHS) in DMSO-d_6, and (c) poly(4-(4-bromophenyloxy)styrene (C) in $CDCl_3$ (run 1, Table 1).

2.2.3 Williamson etherification reaction of poly(4-hydroxystyrene) and 4-bromobenzyl bromide

0.250 g of poly(4-hydroxystyrene) (2.08 mmol of OH functional groups) 0.125 g of NaH 60% dispersion in mineral oil (3.12 mmol) and a stir bar were placed in a two-neck round-bottom flask and attached to the vacuum line. 25 mL of THF was distilled into the flask. The polymer and base were allowed to react until a characteristic light orange color was seen indicating the formation of the phenoxide. At this point, the round-bottom flask was removed from the vacuum line, connected to a reflux condenser, and quickly put under a blanket of argon gas. Separately, 1.04 g of bromobenzyl bromide (4.16 mmol) was dissolved in 10 mL of THF in a septa-capped flask under argon gas. The bromobenzyl bromide solution was then transferred by cannula to the round-bottom flask and the solution was brought to reflux for eight hours. The reactor was then allowed to cool to room temperature before the solution was filtered to remove the solid salt byproduct. The salt was rinsed several times with THF to remove any polymer product. Rotary evaporation was used to reduce the volume of the solution before the polymer was precipitated into a large excess of methanol. The poly(4-(4-bromophenyloxy)styrene) (PBPOS) was collected by filtration and dried in a vacuum oven. (Yield > 72%)

2.3. Chemical and thermal property characterization of synthesized homopolymers

The analysis of all ^{1}H-NMR spectra were performed on a Varian VNMR 500 MHz spectrometer using $CDCl_3$ or DMSO-d_6 as the solvents. Molecular weights were determined using an RI detector based on calibration with polystyrene standards (6000-7500000 Da) by size exclusion chromatography (SEC) measurements performed using a Tosoh EcoSEC System equipped with two Tosoh TSKgel SuperMultiporeHZ-M and one TSKgel SuperMultipore HZ-M guard column. All polymers were eluted with THF at 40 °C with a flow rate of 0.35 mL/min and a run time of 15 minutes. UV-vis spectrophotometry was performed in the wavelength interval 250-900 nm using a Thermo Scientific Evolution 600 UV-Vis Spectrometer using a quartz cuvette. Thermogravimetric analysis was performed on a TA Instruments Q-50 TGA. The sample was heated from 25 °C to 800 °C at a rate of 20 °C/min in the presence of compressed air (Airgas) at a flow rate of 40 mL/min. FT-IR analysis was carried out for functional group characterization.

2.4. Self-assembly of homopolymers in solvent mixtures and its characterizations

In clean dry vials, poly(4-hydroxy styrene) and poly(4-(4-bromophenyloxy)styrene) were dissolved in methanol and THF, respectively, to a concentration of 10 mg/mL and used as a stock solution. All solvents used were freshly filtered and centrifuged at 20,000 RPMs for 30 min to ensure purity. Vials were filled with the desired ratio of solvent mixtures before 0.5 mL of stock solution was added dropwise with vigorous shaking in 5 mL solvents. Visual changes in the turbidity of the solution were used as an indication of the development of particles in the solution. Vials were left unperturbed overnight to allow for settling of the solution.

Dynamic light scattering was used to determine the hydrodynamic radius R_H of polymer particles in solution using a PD Expert Instrument (Precision Detectors) with ten repetitions performed at a scattering angle of 95 degrees. Atomic force microscopy (AFM) samples were drop-cast either onto freshly cleaved mica or onto clean glass slides depending on the microscope used. The samples were spin-coated (1200 rpm) on hydrophobic silica substrate for atomic force microscope (AFM) (Nanoscope IIIa Microscope with Multimode Controller (Veeco Instrument) in tapping mode at room temperature) and field emission scanning electron microscope (FE-SEM, Hitachi S-4700, Japan**)** measurements performed using a

tapping mode at room temperature. Measurements utilizing glass slides as the stage were performed using an Asylum Research MFP3D in contact mode at room temperature for AFM analysis. Transmission electron microscope (TEM) images were obtained using a Zeiss Libra 200 MC TEM/STEM. TEM samples were prepared by depositing 10 µL of vesicle solution onto a carbon-coated copper grid and allowing the solution to dry for several hours (without staining for PBPOS and PHS aggregates sample was stained with I_2 vapor for 6 hours and then dry for another 12 hours). UV-vis spectrophotometry was performed at 250-900 nm wavelength intervals using a Thermo Scientific Evolution 600 UV-Vis Spectrometer using a quartz cuvette.

2.5. As a template for the formation of gold nanoparticles

1 mL of vesicle solution was taken and placed in clean, dry vials to which the appropriate amount of $HAuCl_4$ (the molar ratio of phenol group: Au^{+++} is 1.00:0.25) was added and allowed 6 hours to fully disperse in the vesicle solution. Hydrazine was then added to reduce the HAuCl4 in the solution, which caused a color shift from a yellow solution to a purple or purplish-red solution. The vials were allowed to sit overnight before UV-vis spectroscopy was performed on the solutions.

2.6. Preparation of doxorubicin-loaded poly(4-hydroxystyrene) vesicles

5 mg of doxorubicin hydrochloride was converted to the free base doxorubicin by dissolving in 5 mL of DMSO and reacting with a 2.0 molar equivalent of trimethylamine for 24 hours. 50 µL of a free base doxorubicin solution (50 µg) was added to 2.5 mL of methanol and 0.5 mL of a stock solution of PHS 4 in methanol (10 mg/mL). 7 mL of deionized water was slowly added to the solution. The sample was shaken vigorously and allowed to settle overnight. An analogous solution of poly(4-hydroxystyrene), PHS, (run 4, table 1) vesicles was formed in the same 70/30 v/v ratio of water/methanol to serve as a model for comparison. Both solutions were loaded into a dialysis bag with a molecular weight cut off of 3,500 g/mol and stirred in deionized water for 48 (after 12 hours DI water was changed) hours to remove any free doxorubicin and methanol. These aqueous solutions were used directly for cancer cell treatments at physiological pH of 7.4. The hydrodynamic size was measured by DLS and morphologies was characterized by transmission electron microscope.

2.7. *In-vitro* release of doxorubicin at different pH

For the release of doxorubicin, drug-loaded vesicles were put into a dialysis bag (cut of 3500 g/mole) and release kinetics was observed at pH 4.0, 7.4, and 10.0, respectively. Quantification of doxorubicin was carried out using UV-vis spectrophotometer at 490 nm.[49]

2.8. 3-(4,5-dimethylthiazol-2-yl)-2,5-diphenyltetrazolium bromide and Cell Culture

MTT cell viability assays. The effects of the PHS vesicles with and without loaded DOX (after dialysis) on cell proliferation of HCT-116 cell lines were performed using 3-(4,5-dimethylthiazol-2-yl)-2,5-diphenyltetrazolium bromide (MTT) cell viability assays and it was compared with free DOX and untreated cell line by the reduction of MTT to formazan. HCT-116 cells were seeded (2000 cells/well) in 96 wells plates, after overnight incubation cells were treated with varying concentrations of PHS vesicles for 24 and 72 hours or vehicle (0.1 % DMSO). Then MTT reagent was added to the medium in each well and incubated for 4 hours at 37 °C. Then, reduced formazan crystals were solubilized in DMSO, and optical density values were measured at 540 nm on a microplate reader. All treatments were performed in triplicate and results were expressed as mean ± SE.

HCT-116's, a colon cancer cell line, were counted and seeded at 100,000 per 60 mm2 dish with Dulbecco's Modified Eagle Medium (DMEM) supplemented with 10% Fetal Bovine Serum (FBS) and 5 mM Glucose. Briefly, the cells were trypsinized, pelleted, and counted using an automated cell counter, Cell Scepter 2.0 EMD Millipore according to manufacturer instructions. Cells were left to grow over 24 hours before beginning treatment.

2.9. Treatment of HCT-116 cancer cells with Doxorubicin-loaded Poly(4-hydroxystyrene) vesicles

Vesicles with and without doxorubicin were mixed separately with cells in culture media in a 1:1 ratio with phosphate buffer saline at physiological pH 7.4. 500 µL of the PBS solution was added to 4.5 mL of cell culture media (as described above) to give a final concentration of 41,000 vesicles per 5 mL of media or ~8,000 vesicles per mL (The initial number of vesicles was 82000 vesicles/mL, observed). Treatments were left on for 24 hours and completed in duplicate. At the end of this time point cells were trypsinized, pelleted, and re-counted.

3. Results and discussion

3.1. Characterizations of poly(4-(1-ethoxyethoxy)styrene), poly(4-hydroxystyrene), and poly(4-(4-bromophenyloxy)styrene

Well-defined homopolymers of poly(4-(1-ethoxyethoxy)styrene) were synthesized by anionic polymerization at -98 °C using high vacuum techniques, followed by cleavage of the acetal protecting group to yield the poly(4-hydroxystyrene) with the controled molecular weight. Subsequently, the poly(4-hydroxystyrene) was reacted with 4-bromobenzyl bromide, in Williamson etherification reaction for the synthesis of poly(4-(4-bromophenyloxy)styrene) (Fig.1). The results of the polymerization and subsequent post-polymerization modification steps are summarized in Table 1. Insight into the molecular structure of the polymers was achieved through ^{1}H-NMR spectra (Fig. 1a-c). The observed number of average molecular weight (M_n), calculated molecular weight, and polydispersity index (PDI, M_w/M_n) are shown in Table 1 and SEC chromatograph profile is shown in Fig. 2a. The observed M_n and PDI were measured by SEC. The anionic polymerization of 4-(1-ethoxyethoxy)styrene and acidic deprotection had previously been recorded in the literature so the structure of these homopolymers was confirmed with the previously reported ^{1}H-NMR spectra.[26] The quantitative conversion of PHS to PBPOS was confirmed by the disappearance of the hydroxyl singlet peak at 9.0 ppm (Fig. 1b) and the integration of a newly developed singlet at ~4.90 ppm (Fig. 1c) corresponding to the methylene protons and the two additional

broad singlets between 7.5 ppm and 7.0 ppm corresponding to the four additional aromatic protons (Fig. 1c) with the support of FT-IR data (C-Br bands) and thermal data of the homopolymers.

Further confirmation was seen in the FT-IR spectra of both polymers as the broad OH stretch apparent in the spectra of poly(4-hydroxystyrene) disappears in the spectra of poly(4-(4-bromophenyl oxy)styrene) and presence of the C-Br vibration peak at 1008 cm^{-1} and C-Br stretching bands at 682 cm^{-1} support the NMR spectra of PBPOS (Fig. 2b). The Williamson etherification reaction of PHS was achieved with similar ease to the analogous small molecule reaction of phenol. The possibility of directly synthesizing a targeted molecular weight and narrow molecular weight distribution PBPOS by anionic polymerization of the 4-bromophenyloxy styrene is dubious due to the likelihood of lithium halogen exchange reactions. The exchange reaction would likely cause crosslinking and carbanion species in the solution of different reactivities.

Characterization of the thermal properties of all three polymers, PpEES, PHS, and PBPOS was conducted using TGA and DSC. The decomposition temperature (T_d) values were determined at 5% weight loss. As expected, PHS exhibits a single-step thermal degradation with a Td temperature of ~350 °C, consistent with what is reported works.[50] The polymers PBPOS and PpEES both show a two-step thermal degradation, although the effect is significantly more pronounced in PpEES (Fig.S1†). The T_d values for PpEES and PBPOS were 291 °C and 300 °C, respectively.

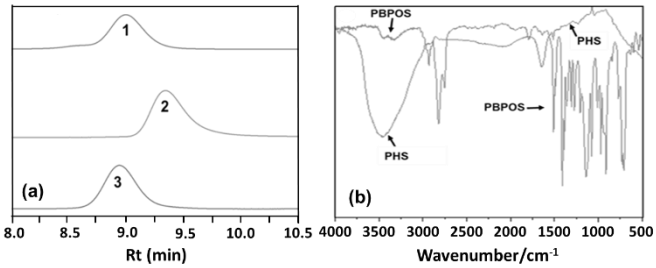

Fig. 2 (a) SEC traces for the conversion of poly(4-(1-ethoxyethoxy) styrene) (PpEES) (1) to poly(4-hydroxystyrene) (PHS) (2) to poly(4-(4-bromophenyloxy)styrene) (PBPOS) (3) (run 4, Table 1) in THF, and (b) FT-IR spectra of PHS and PBPOS (run 4, Table 1)

In the thermal decomposition of PpEES, approximately 30 % weight loss occurs in the first step which corresponds to the weight percentage of the acetal-protecting group. Therefore, thermal deprotection of the acetal group can be assumed to occur upon annealing the polymer at an elevated temperature (above 291°C). For PBPOS, the onset of the first and second steps of decomposition are too close to make this type of observation. DSC was used to determine the T_g of the new homopolymer and was observed to be between 58 °C and 67 °C (Fig. S2†).

Table 1. Molecular Characteristics of Amphiphilic homopolymers Poly(4-hydroxystyrene) and Poly (4-(4-bromophenyloxy)styrene)

Run	Sample	Initiator (mole x 10^{-4})	Monomer (mole x 10^{-4})	Polymer	$M_{n,(obs)}$ (g/mole)	$M_{n,(calc)}$ (g/mole)	PDI M_w/M_n	Yield (%)
1	1a	2.0	72.6	PpEES	6000	7000	1.01	87
	1b			PHS	4800		1.11	
	1c			PBPOS	9870		1.10	
2	2a	1.0	53.0	PpEES	9250	10200	1.06	98
	2b			PHS	5400		1.11	
	2c			PBPOS	13800		1.09	
3	3a	1.0	73.0	PpEES	10800	10900	1.07	98
	3b			PHS	5800		1.14	
	3c			PBPOS	17000		1.21	
4	4a	1.0	55.9	PpEES	14600	14100	1.06	99
	4b			PHS	9400		1.08	
	4c			PBPOS	21500		1.17	

Note: poly(4-(1-ethoxyethoxy)styrene) (PpEES) synthesized by anionic polymerizatiion, poly(4-hydroxystyrene) (PHS) synthesized by deprotection of PpEES and poly(4-(4-bromophenyloxy)styrene) (PBPOS) synthesized by Williamson Etherification Reaction of PHS and 4-bromobenzyl bromide, yield of the reaction was more than 95% in each case. M_n(obs) and M_w/M_n were obtained by SEC.

Polymer Chemistry

Paper

3.2. Self-assembly behaviours of homopolymer

The self-assembly behaviours of PHS, and PBPOS, were observed in selective solvents. The flexible vinyl backbone of homopolymers PHS and PBPOS are hydrophobic, whereas, the rigid pendent group of homopolymer PHS and PBPOS are relatively more hydrophilic making these homopolymers amphiphilic. The inter-competition between the backbone and pendent groups in a selective solvent composition is expected to be responsible for the self-assembly behaviours (Scheme 1). The aggregation behaviours of PHS were investigated in the mixed solvent of H_2O and methanol, H_2O and THF, and hexanes and THF at different solvent ratios (v/v). It is expected that the hydroxyphenyl moiety of the PHS is acting as a donor to interact with water through hydrogen bonding (Scheme 1).

The self-assembly behaviours of PHS were investigated in H_2O: THF and H_2O: MeOH mixed solvent as an aqueous dispersion at different compositions (v/v). The hydrodynamic size of the aggregates of the PHS in different solvent compositions is shown in Fig. 3. In general, decreasing the water percentage in H_2O: THF mixed solvent (up to H_2O: THF ratio 60:40 (v/v)), the size of the aggregates remains constant at the statistical range. However, at the H_2O: THF ratio of 50:50 (v/v), the size of the PHS aggregates increased by 3-fold (Fig. 3a). For solvent mixtures of H_2O: MeOH, a similar trend was observed for PHS up to H_2O: MeOH ratio 70:30 (v/v) (size slightly increased) and at the H_2O: MeOH ratio 60:40 (v/v), aggregates size increased from ~110 to ~320 nm (Fig. 3 b). No remarkable effect of molecular weight on aggregate size was observed (Figs.3a and 3b). In the case of PBPOS, after 30% of THF content in water, the size of aggregates decreased remarkably which is the opposite trend of the PHS aggregates (Fig. 3c). This indicates that the polarity of the pendent groups along with the polarity of a solvent mixture play a role in the aggregation behaviours of the homopolymers

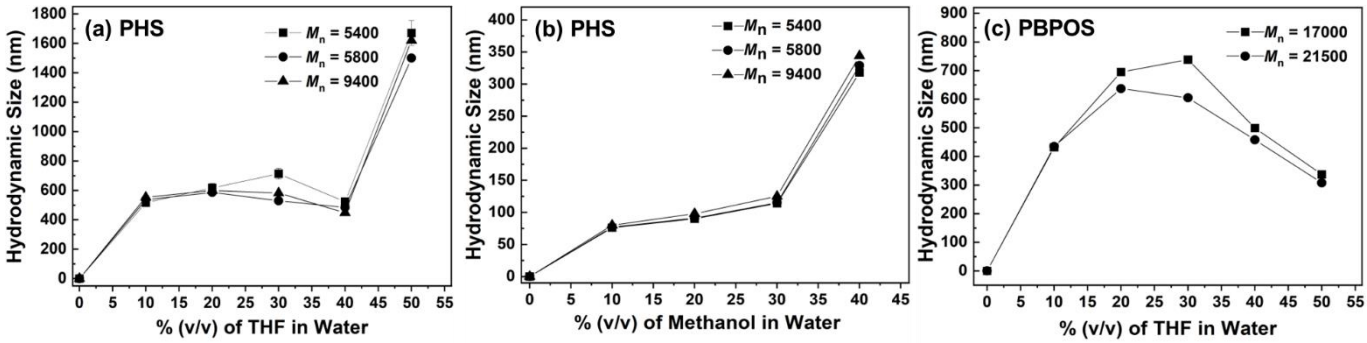

Fig. 3 Hydrodynamic size of the poly(4-hydroxystyrene)(PHS) aggregates in (a) different compositions of water: THF mixed solvent, (b) different composition of water: methanol mixed solvent, and (c) hydrodynamic size of the poly(4-(4-bromophenyloxy)styrene) (PBPOS) aggregates in water: THF mixed solvent.

Figs. 4a and 4b represent scanning electron microscope (SEM) and transmission electron microscopy (TEM) images, respectively, of the PHS aggregates formed from H_2O: THF (60/40, v/v) azeotropic solvent (AFM micrographs shown in Fig. 3Sa†). Figs. 4c and 4d, respectively represent scanning electron microscope (SEM) and transmission electron microscopy (TEM) images, of the PHS aggregates formed from water: THF (50:50, v/v) azeotropic solvent (AFM micrographs shown in Fig. 3Sb†). The TEM images Fig. 4b and 4d show the contrast differences in the centre and periphery in Fig. 4b d, which is a characteristic of hollow spheres.[51] For further confirmation of the hollow nature, static light scattering (SLS) measurements were carried out at room temperature to measure the average radius of gyration (R_g) of the micelles and vesicles. The ratio R_g/R_h (where R_h = 0.5 × hydrodynamic size) is useful for the characterization of the nanostructure.[14] The Rg/R_h ratio was near to 0.991 for PHS aggregates in H_2O: THF azeotropic solvent which indicates a hollow sphere has been formed which is in correlation with TEM micrographs of Fig. 4 b and 4d.

The size of aggregates observed from SEM and TEM images is roughly 35% smaller than hydrodynamic size**.** From 10 to 30% THF in water (v/v), the size of the hollow aggregates is roughly equivalent within the ± 30 nm range. However, at 60:40 (v/v) H_2O: THF solvent composition, 3 times increase in the size of the aggregates was observed (Fig. 3a) by dynamic light scattering, mainly due to the association of aggregates (Figs. 4c and 4d).

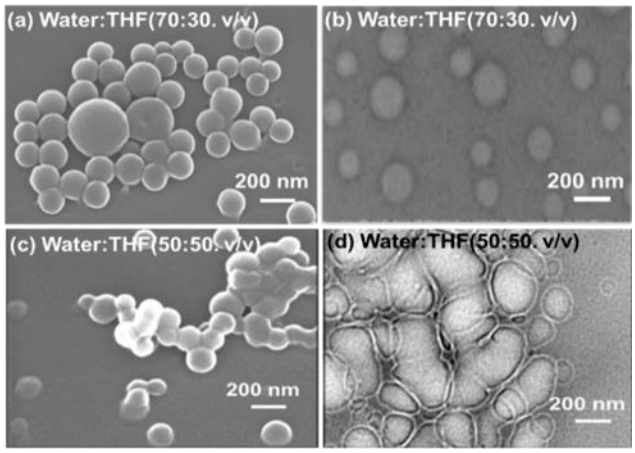

Fig. 4 Morphologies of poly (4-hydroxystyrene) (PHS), (Mn = 9400 g/mole, run 4 (Table 1) (a) scanning electron microscope (SEM) micrograph image of PHS in a mixed solvent of water: THF (70:30, v/v), (b) transmission electron microscope (TEM) micrograph of PHS in **a** mixed **solvent** of water: THF (70:30, v/v), (c) SEM micrograph of PHS in **a** mixed **solvent** of water: THF 50:50, v/v), and, (d) TEM micrograph of PHS in mixed solvent of water: THF (50:50, v/v).

A similar trend was observed for H_2O: MeOH mixed solvent but the size of the aggregates was smaller than for H_2O: THF solvent compositions (Fig.3b, Fig.5). Interestingly, at 70:30 H_2O: MeOH solvent composition (v/v), 3 times increase in size is due to association of aggregates (DLS data of Figure 3b), SEM micrograph of Fig. 5c, and TEM micrograph of Fig. 5d). This indicates that the overall polarity of the solvent influences the aggregation behavior of PHS. THF is also a good solvent for the vinyl backbone of the PHS, whereas, methanol and water are unfavorable.

In such cases, solvation of the homopolymer by THF resulted in less curvature in the vinyl (coil) backbone. As a result, larger hollow micelles were observed than in H_2O: MeOH mixed solvent (Figu**re** 3b, Scheme 1a). However, as per solvent chemistry, the possibility of the formation of bilayer layer vesicles is more acceptable in an H_2O: MeOH mixed solvent. For further observation, PHS aggregates in H_2O: MeOH (70:30, v/v) mixed solvent were used as the template for the formation of gold nanoparticles (detailed procedure of synthesis of Au nanoparticles shown in Supporting Information Fig.S3† and TEM micrographs of aggregates with Au nanoparticles shown in Fig. 5e. The phase contrast at the center and peripheries along with the presence of collapsed aggregates indicate the vesicular nature of the PHS aggregates in H_2O: MeOH mixed solvent. Also, the R_g/R_h ratios were in the range of 0.89 - 0.91 for PHS aggregates in H_2O: MeOH mixed solvent that indicates vesicle characteristics.[14,52,53]

The orientation of the 4-hydroxyphenyl pendent groups can be predicted by the location of Au nanoparticles. During the nucleation process of Au nanoparticles, the size of nanoparticles depends on intermolecular force among capping agent and nanoparticles, nanoparticles-nanoparticles, and nanoparticles-solvent molecules. In the present case, methanol is closer to PHS pendent groups due to its chemical nature (indicated by the solubility of PHS in methanol), which is a nucleation site of Au nanoparticles. It is reported in the literature that methanol favors more nucleation of Au atoms and results in the association of small to larger nanoparticles, which is visible in Fig.S4a-b†.

The UV-vis spectra show a broad plasma band from 535 to 610 nm range (Fig. S5†). The presence of Au nanoparticles on the surface of vesicles as well as inside of the vesicles (Fig. 5e and Fig. S4a-b†), supports the argument for the formation of bilayer vesicles with 4-hydroxyphenyl pendent groups facing the water solvent both inside and outside as shown in Scheme 1a.

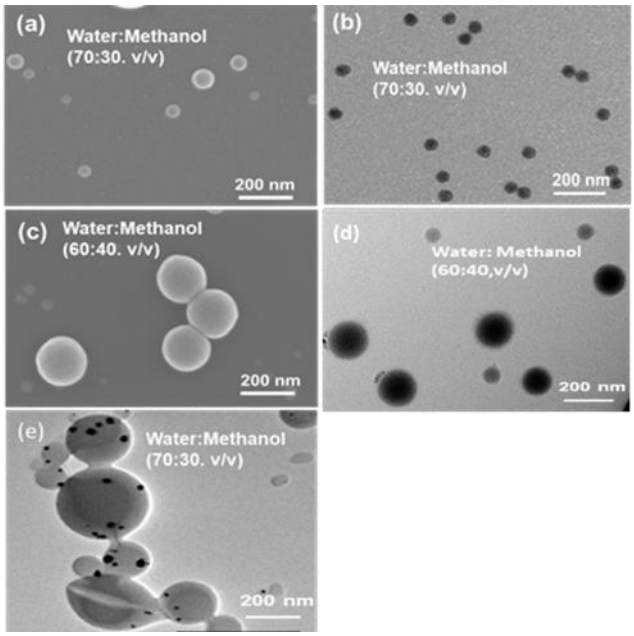

Fig. 5 Morphologies of poly (4-hydroxystyrene) (PHS), (Mn = 9400 g/mole, run 4 (Table 1)) (a) scanning electron microscope (SEM) micrograph image of PHS in a mixed solvent of water: methanol (70:30, v/v), (b) transmission electron microscope (TEM) micrograph of PHS in a mixed solvent of water: methanol (70:30, v/v), (c) SEM micrograph of PHS in mixed solvent of water: methanol (60:40, v/v), (d) TEM micrograph of PHS in mixed solvent of water: methanol (60:40, v/v), and (e) TEM micrograph of gold nanoparticle synthesized in PHS vesicles (water: methanol = 70:30, v/v).

In an analogous manner to the hydrogen bonding of PHS, the bromobenzene head group of PBPOS participates in halogen bonding. Halogen bonding is a non-covalent attraction that occurs between a covalently bonded halogen atom (donor) and a nucleophile (acceptor). Due to the anisotropic electron density of a bound halogen atom, a belt of predominantly negative electrostatic potential forms orthogonal to the bond direction and is offset by a predominantly positive region on the end.[54] The effect of the predominant positive end is referred to as the σ-hole and is more frequently observed in the heavier halogens (Br, I). In the case of PBPOS, the bromobenzene head group acts as the halogen bond donor, and the electron-dense oxygen atom of water acts as the acceptor. The strength of this interaction coupled with the hydrophobicity of the hydrocarbon backbone is the driving force of the self-assembly of these homopolymers. TEM imaging of the polymer vesicles of PBPOS in a mixed solvent of water and THF (70:30, v/v) required no staining due to the higher contrast provided

by the bromine atoms. The bromine atoms appear to be on the surface of the vesicles as would be predicted if halogen bonding were the driving force of the self-assembly (Fig. 6). Fig.6a shows the AFM phase contrast image of the PBPOS vesicles and corresponding TEM micrograph shown in Fig.6b.

The nature of the self-assembled aggregates in the solution was investigated by AFM, as shown in Fig.6a. The surface of the aggregates appears to be rough rather than smooth with what appear to be smaller vesicles partaking in either fusion or fission with the larger aggregate. For vesicles in solution, fission and fusion are dynamic processes and the time lag between the fission process and response of the homopolymer chain probably plays a role in open-mouth vesicles of PBPOS (Figs. 6b).[13-15]

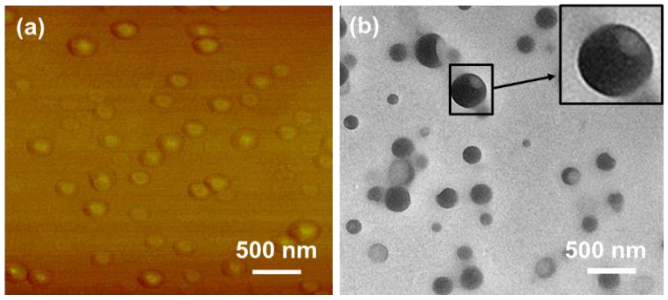

Fig. 6 (a) AFM, (b) TEM micrographs of poly(4-(4-bromophenyloxy) styrene) (PBPOS, Mn= 21500 g/mole) in a water: THF mixed solvent (70:30, v/v, Inset micrographs are selected area images).

3.2.1. Mechanism of the self-assembly

In PHS and PBPOS amphiphilic homopolymers, the vinyl backbones have the characteristics of a coil nature, which is essential to form a curvature to make a spherical aggregate. Herein, for H_2O: THF mixed solvent, THF forms an azeotrope containing 5.8% v/v of water molecules.[55] Intermolecular interaction between a THF and a water molecule in an azeotrope is stronger than the interaction among THF-THF molecules or water-water molecules. In amphiphilic homopolymer PHS, water-THF azeotropic solvent, water molecules interact with the 4-hydroxyphenyl group of the polymer chain due to the stronger attraction and it acts as a separator of water molecules from the azeotrope (Scheme 1a) into three layers: THF (near vinyl group), THF-water azeotrope (near to 4-hydroxyphenyl group), and bulk water.[55] In the present case, the majority of THF molecules can be considered as free and a minor solvent, which is inside the hollow micelles (Scheme 1a, Fig.3b), whereas the water molecules are outside of the hollow micelles.[56] This indicates that the competition between flexible vinyl backbone coil and rigid pendant group in a selective solvent is responsible for forming well-shaped aggregates like lipids, small surfactant molecules, or block copolymer aggregates. However, in the case of amphiphilic homopolymer, it is only possible by tangential packing of molecules in an aggregate (Scheme 1), which is different than the lateral packing seen in block copolymer aggregates.

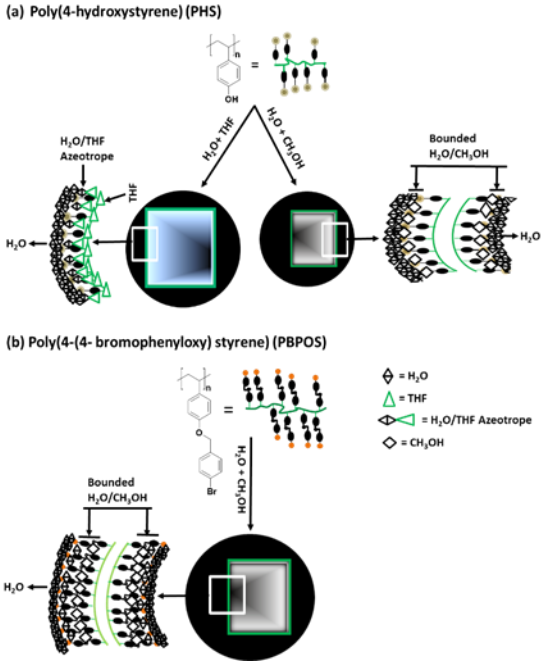

Scheme 1. Systemizing sketch for micelles and vesicles from (a) poly(4-hydroxystyrene) and (b) poly(4-(4-bromophenyloxy)styrene) (PBPOS).

The molecular weight of amphiphilic homopolymer does not much affect the size of the aggregates (Fig. 3). The formation of a curved structure suggests that the molecular rotation of the sigma bond between vinyl carbon and the pendent group of the amphiphilic homopolymer freezes due to the formation of the noncovalent bonds (hydrogen/halogen bonds) between the required solvent molecules and pendent group oriented towards the favorable solvent side to form well shape nano-aggregates. Form and entropy consideration for the formation of well-shaped aggregates from the

amphiphilic polymeric systems, the polymer must provide the required area of curvature with proper orientation to adjust the packing parameter to form stable aggregates. Experimental data from Figs. 3 to 6 suggest that PHS or PBPOS, possibly rearranging tacticity to an isotactic arrangement (Scheme 1) due to the presence of a sigma bond in vinyl and the bond between the vinyl and pendent group, molecular rotation is allowed.[13,14]

3.3. Doxorubicin loading and in-vitro drug release

Doxorubicin (DOX) is a common chemotherapy drug used for the treatment of several variants of breast, lung, colon, and many other cancers.[57,58] DOX is a water-soluble molecule, with an orange-red color at neutral pH. It is commonly sold in the more aqueous soluble doxorubicin HCl salt. To encapsulate it in the hydrophobic vesicle layer, the salt must be reduced to a free base. Doxorubicin HCl (DOX HCl) is converted to the free base by reaction with triethylamine (TEA) in a 1:2 molar ratio of DOX HCl overnight in DMSO. 50 µL of the DOX/DMSO was added to 2.5 mL of methanol followed by 0.5 ml of PHS solution at 10 mg/mL and thoroughly mixed. To this mixture, 7 mL of DI water was added to produce the formation of polymer vesicles. The mixture was dialyzed for 48 hours to remove non-encapsulated DOX. A visual inspection of the samples shows the presence of the red-orange color of doxorubicin in the solution after dialysis has been performed (Fig. S6†). An analogous vesicle solution without DOX was prepared to compare the particle size by DLS (Fig. S7†). and morphologies observed by TEM (Fig. S8†). *In-vitro* drug release was observed in phosphate buffer saline at pH, 4.0, 7.4, and 10.0 at a physiological temperature of 37 °C (Fig.7a). Drug release from PHS vesicles, depends on the pH of the media, at pH 10.0 rate of drug release was higher than at lower pH.

The DLS measurements were performed on the dialyzed solutions, revealing an increase in particle size for the solution with vesicles loaded with DOX relative to the empty vesicles. The average hydrodynamic diameter of the PHS vesicles was found to be 71 nm (Fig. S7c†) for DOX loaded system and 55 nm (Fig S7b†) for empty vesicles in the aqueous suspensions, which correlates with transmission electron microscope micrographs (Figs. S8a† and S8b†). The size of vesicles after dialysis against water was smaller than vesicles in H_2O: MeOH mixed solvent (70:30, v/v) (Fig. 3b and Fig. S7a†). In a basic environment, the phenolic hydrogen is likely removed to form a phenoxide group within the polymer chain and a release rate of DOX was observed.[32] The solubility of phenoxide in aqueous solutions is higher than the phenol group (relatively stronger interaction), allowing for more curvature in the vinyl backbone to form smaller size vesicles. This also suggests that at neutral pH, the phenol group is probably facing methanol molecules as shown in Scheme 1a.

3.4. MTT and Cell culture

Data from MTT experiment is shown in Fig.7b. In comparison to untreated samples, roughly 35% less viable HCT-116 cell was observed after treatment with DOX-loaded PHS vesicles. For cell treated with PHS vesicles without DOX loading show near 87 % cell viability. The viable value of more than 90 % is considered nontoxic.[19]

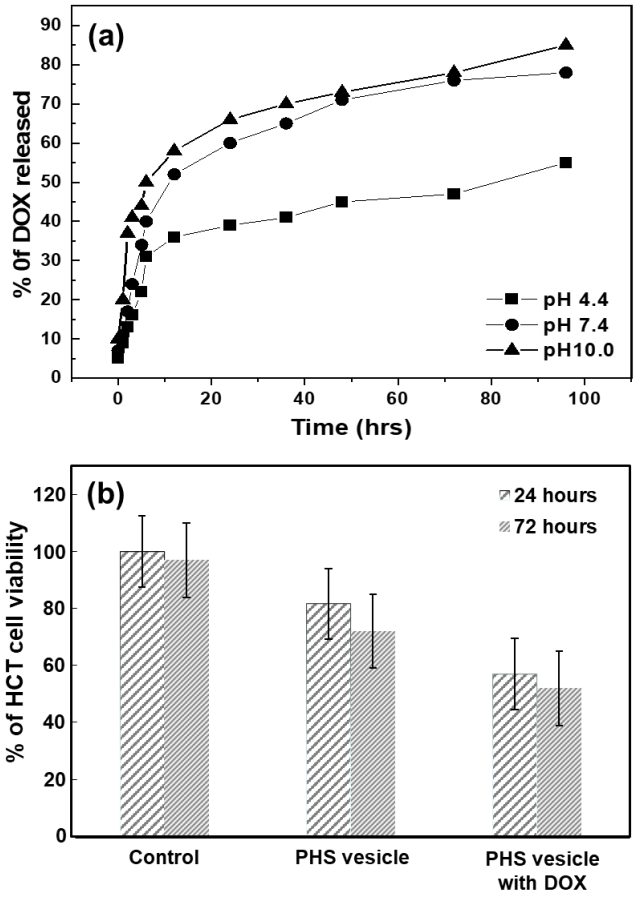

Fig. 7 (a) *In-vitro* release of DOX from PHS vesicle and (b) cell viability data by MTT method for untreated cells (control), empty vesicle treated , and DOX loaded vesicle treated HCT-116 cell (24 and 72 hours), respectively.

The HCT-116 cells, a colon cancer cell line, were maintained in normoxia incubator conditions (37°C, 95% Air, 5% CO_2) experimental testing with DOX-loaded vesicles. The treatment of empty vesicles was intended to account for any cytotoxic quality that might be inherent in the polymer itself. The 3% difference in cell count suggests that the poly(4-hydroxystyrene) has slight cytotoxicity (Fig.S9b†) in comparison to the control sample (Fig.S9a†). After 24 hours, the population of HCT-116 cells treated with vesicles loaded with DOX saw a 27% lower cell count than the untreated cells and 24 % lower than the cells treated with empty vesicles. (Table 2) (Fig.S9c†).

Table 2. HCT-116 cell counts 24 hours after treatment with DOX-loaded poly(4-hydroxystyrene) vesicles.

Cell Treatment	Average CellCount[a]	% Change[b]
Untreated	263,950	0
Without DOX empty PHS vesicle	254,800	-3
With DOX loaded PHS vesicle	189,900	-27

Note: [a]average of three experiments; [b]% change based on the direct population comparison with the untreated cells.

A decrease in the cell counts with PHS control vesicles suggests that phenol/phenoxide group of the PHS interacts with cancer cell membrane chemical groups such as protein, lipids, carbohydrates, and its derivatives either through hydrogen bonding or charge attraction, which can help, PHS vesicles to penetrate the cell membrane and release the drug inside the cell.

4. Conclusions

The anionic polymerization of 4-(1-ethoxyethoxystyrene) at -98 °C yields polymers with predictable molecular weights and narrow polydispersity index. The cleaving of the acetal protecting group at room temperature produces the homopolymer poly(4-hydroxystyrene). The Williamson etherification reactions performed with poly(4-hydroxystyrene) and 4-bromobenzyl bromide quantitatively yield the new polymer poly(4-(4-bromophenyloxy) styrene). The new polymer exhibits values of T_g between 57 °C and 67 °C. The strategy of accessing functionalized polystyrene by etherification reaction of poly(4-hydroxystyrene) and alkyl bromide species could be adapted for the synthesis of numerous polymers. Homopolymer self-assembly of PHS and PBPOS in aqueous mixture was driven by the intra and intermolecular forces of hydrogen bonding and halogen can be used to form nanoaggregates of predesigned size and shape in selective solvents. The poly(4-hydroxystyrene) vesicles show a potential as a template for the formation of metal nanoparticles and reservoirs of pharmaceutically active molecules. The rate of release of pharmaceutically active organic molecules depends on the pH of the media. Doxorubicin-loaded poly(4-hydroxystyrene) is effective against the HCT-116 cancer cell. Like hydrogen bonding, halogen bonding can be used to form nano aggregates of predesigned size and shape in selective solvents. Poly(4-hydroxystyrene) and its derivative micelles or vesicles can be used for the removal of cations (inorganic or organic) from desired solvents.

Acknowledgements

This research leading to these results has received funding from Ministry of Higher Education, Research and Innovation (MoHERI) of the Sultanate of Oman under Bulk Funding Program with Agreement Number MoHERI/BFP/UOB/RG01/2022. A portion of this work was supported by a user project at the Centre for Nano phase Materials Sciences supported at Oak Ridge National Laboratory by the U. S. Department of Energy.

Conflict of Interest

There is no conflict of interests

References

1 J. Zhang, K. L Liu, K.; Mullen, and M. Z. Yin, Self-assemblies of amphiphilic homopolymers: synthesis, morphology studies and biomedical applications, *Chemical Communications,* 2015, 51, 11541-11555.

2 R. C. Hayward, D. J. Pochan, Tailored Assemblies of Block Copolymers in Solution: It Is All about the Process, *Macromolecules*, 2010, 43, 3577-3584.

3 G. Odian, Principles of Polymerization; 4th ed.; John Wiley & Sons, Inc.: Hoboken, New Jersey, 2004.

4 K. Kataoka, A. Harada, Y. Nagasaki, Block copolymer micelles for drug delivery: Design, characterization and biological significance, *Advanced Drug Delivery Reviews*, 2012, 64, 37-48.

5 C. Weber, R. Hoogenboom, U. S. Schubert, Temperature responsive bio-compatible polymers based on poly(ethylene oxide) and poly(2-oxazoline)s, *Progress in Polymer Science,* 2012, 37, 686-714.

6 L. C Gilday, S. W, Robinson, T. A. Barendt, M. J. Langton, B. R Mullaney, P. D Beer, Halogen bonding in supramolecular chemistry, *Chem. Rev.,* 2015, 115, 7118–7195

7 S. Basu, D. R. Vutukuri, S. Shyamroy, B. S. Sandanaraj, and S. Thayumanavan, Invertible Amphiphilic Homopolymers, *J. Am. Chem. Soc*., 2004, 126, 9890-9891.

8 N. G. Kang, M. Changez, J. S. Lee, Living Anionic Polymerization of the Amphiphilic Monomer 2-(4-Vinylphenyl)pyridine, *Macromolecule*s, 2007, 40, 8553-8559.

9 K. Yoshihiko and T. Takaya, Morphology transition of amphiphilic homopolymer self-assemblies in water triggered by pendant design and chain length, *European Polymer Journal*, 2020, 139, 110001.

10 T. Kubo, C. P. Easterling, R. A. Olson, and B.S. Sumerlin, Synthesis of multifunctional homopolymers via sequential post-polymerization reactions, *Polym. Chem.,* 2018, 9, 4605-4610.

11 P. Xuefengm, K. Zdravko, W. Yong-Lei, M. S. Radwan, H. Eneli, G. Siddharth, S. Sasho, A. E-N. Gumaa. T. M. Matthew, S. Robin, D. Jérôme, G. Christian, Y. Jiayin, and L. Yan, Poly(ionic liquid) nanovesicles via polymerization induced self-assembly and their stabilization of Cu nanoparticles for tailored CO_2 electroreduction, *J. Colloid and Inter. Sci.,* 2023, 637, 408-420.

12 S. Swan, F. O. Egemole, S. B. T.; Nguyen, and J. H. Kim, Assembly of Short-Chain Amphiphilic Homopolymers into Well-Defined Particles, *Langmuir,* 2020, 36, 16, 4548-4555.

13 M. Changez, N. G. Kang, C. H. Lee, and J. S. Lee, Reversible and pH-Sensitive Vesicles from Amphiphilic Homopolymer Poly(2-(4-vinylphenyl) pyridine), *Small,* 2010, 6, 63-68.

14 M. Changez, N. G. Kang, and J. S. Lee, Uni-molecular Hollow Micelles from Amphiphilic Homopolymer Poly(2-(4-vinylphenyl) pyridine), *Small*, 2012, 8, 1173-1179.

15 Y. H. Hur, N. G. Kang, B. G. Kang, Y. G. Yu, M. Changez, and J. S. Lee, Novel amphiphilic homopolymers containing meta- and para-pyridine moieties with living characteristics and their self-assembly, *J. Polym. Sci. Pol. Chem*., 2013, 51, 3458-3469.

16 R. R. Rajsekher, P. Prasad, A. Finne, and S. Thayumanavan, Zwitterionic amphiphilic homopolymer assemblies, *Polym. Chem.*, 2015, 6, 6083-6089.

17 Y. Kimura, M., Takenaka, M. Ouchi, and T. Terashima, Self-Sorting of Amphiphilic Block-Pendant Homopolymers into Sphere or Rod Micelles in Water, *Macromolecules*, 2020, 53, 12, 4942-4951.

18 Y. Jang, A. M. Alb, J. B. He, and S. M. Grayson, Neutral linear amphiphilic homopolymers prepared by atom transfer radical polymerization, *Polym. Chem.,* 2014, 5, 622-629.

19 J. Y. Liu, W. Huang, Y. Pang, P. Huang, X. Y. Zhu, Y. F. Zhou, and D. Y. Yan, Molecular Self-Assembly of a Homopolymer: An

Alternative To Fabricate Drug-Delivery Platforms for Cancer Therapy, *Angew. Chem.-Int. Edit*., 2011, 50, 916-9166.

20 J. Z. Du, H. Willcock, J. P. Patterson, I. Portman, and R. K. O'Reilly, Self-Assembly of Hydrophilic Homopolymers: A Matter of RAFT End Groups, *Small,* 2011, 7, 2070-2080.

21 D. J. Yao, T. P. Bender, P. J. Gerroir, P. R. Sundararajan, Self-assembled vesicular nanostructures of perylene end-capped poly (dimethylsiloxane), *Macromolecules*, 2005, 38, 6972-6978.

22 M. Z. Yin, J. Shen, W. Pisula, M. H. Liang L. J. Zhi, and K. Mullen, Functionalization of Self-Assembled Hexa-peri-hexabenzocoronene Fibers with Peptides for Bioprobing, *J. Am. Chem. Soc*., 2009, 131, 14618-14619.

23 J. Zhang, S. S. You, S. K. Yan, K. Mullen, W. T. Yang, and M. Z. Yin, pH-responsive self-assembly of fluorophore-ended homopolymers, *Chemical Communications*, 2014, 50, 7511-7513.

24 X. Ma, Y. Wang, T. Zhao, Y. Li, L.-C. Su, Z. Wang, G. Huang, B. D. Sumer, and J. Gao, Ultra-pH-Sensitive Nanoprobe Library with Broad pH Tunability and Fluorescence Emissions, *J. Am. Chem. Soc*.,2014, 136, 11085-11092.

25 C. Y. Hsu, S. C. Chang, K. Y. Hsu, and Y. L. Liu, Photoluminescent Toroids Formed by Temperature-Driven Self-Assembly of Rhodamine B End-Capped Poly(N-isopropylacrylamide), *Macromolecular Rapid Communications*, 2013, 34, 689-694.

26 A. Natalello, C. Tonhauser, and H. Frey, Anionic Polymerization of para-(1-Ethoxy ethoxy) styrene: Rapid Access to Poly(p-hydroxystyrene) Copolymer Architectures, *ACS Macro Letters,* 2013, 2, 409-413.

27 A. Natalello, M. Werre, A. Alkan, and H. Frey, Monomer Sequence Distribution Monitoring in Living Carbanionic Copolymerization by Real-Time ^{1}H NMR Spectroscopy, *Macromolecules,* 2013, 46, 8467-8471.

28 D. P. Sweat, M. Kim, A. K. Schmitt, D. V. Perroni, C. G. Fry, M. K. Mahanthappa, and P. Gopalan, Phase Behavior of Poly(4-hydroxystyrene-block-styrene) Synthesized by Living Anionic Polymerization of an Acetal Protected Monomer, *Macromolecules*, 2014, 47,6302-6310.

29 D. P. Sweat, X. Yu, M. Kim, and P. J. Gopalan, Synthesis of poly(4-hydroxystyrene)-based block copolymers containing acid-sensitive blocks by living anionic polymerization, *Polym. Sci. Pol. Chem.*, 2014, 52, 1458-1468.

30 N. Hayashi, T. Ueno, S. Hesp, M; Toriumi, and T. Iwayanagi, Tetrahydropyranyl protected polyhydroxy-styrene for a chemically amplified deep uv resist, *Polymer*, 1992, 33, 1583-1588.

31 I. Natsuki, H. Kota, K. Miwa, M. Keitaro, and S. Kazuki, Design of LCST-type phase separation of poly(4-hydroxystyrene), *Mol. Syst. Des. Eng.*, 2023, 8, 79 -84.

32 S. Qiang, Z. Haiyan, J. Jajuan, S. Xiufang, S. Jiankui. X. Yuantao, L. Lihua, C. HuanHuan, S. Yi, H. Guixiang, G. Yuexin, Z. Zhiguo, Poly(styrene-co-4-hydroxystyrene) nanofiber membrane for highly selective and efficient Rb+ capture from high salinity solution, Separation *and Purification Technology* 2023, 312, 123334

33 H. Hsieh, R. P. Quirk, Anionic Polymerization: Principles and Practical Applications; *Marcel Dekker, Inc.:* New York, New York 10016, 1996.

34 N. G. Kang, M. Changez, M. J. Kim, and J. S. Lee, Effect of Biphenyl Spacers on the Anionic Polymerization of 2-(4′-Vinylbiphenyl-4-yl) pyridine, *Macromolecules*, 2014, 47, 6706-6714.

35 A. Hirao, S. Loykulnant, and T. Ishizone, Recent advance in living anionic polymerization of functionalized styrene derivatives, *Progress in Polymer Science,* 2002, 27, 1399 -1471.

36 Z. Rappoport, The chemistry of phenols Parts 1 and 2, Wiley: Hoboken, NJ, 2003, ISBN 0-471-49737-1.

37 K. Muhammad, G. Shabbir, and S. Hameed, Synthesis, Characterization, and Study of Thermal and Liquid Crystalline Properties of Poly(4-(6-(4-vinylphenoxy)hexyloxy)benzoic Acid), *Mole.Cryst. and Liq.Cryst.,* 2012, 569, 40-48.

38 F. C. Rossitto and P. M. Lahti, Solid-state photochemical generation of polymeric polyradicals: Poly(4-vinylphenoxy) and copolymers with styrene, *J. Polym. Sci. Polym. Chem.*, 1992, 30, 1335-1345.

39 G. D. Xu, Y. F. Zhang, R. Rohan, W. W. Cai, H. S. Cheng, Synthesis, Characterization and Battery Performance of A Lithium Poly (4-vinylphenol) Phenolate Borate Composite Membrane, *Electrochim. Acta*, 2014, 139, 264-269.

40 L. Sheng, T. Higashihara, S. Nakazawa, M. Ueda, Polystyrenes containing flexible alkylsulfonated side chains as a proton exchange membrane for fuel cell application, *Polym. Chem.,* 2012, 3, 3289-3295.

41 C. Schull and H. Frey, Controlled Synthesis of Linear Polymers with Highly Branched Side Chains by "Hypergrafting": Poly(4-hydroxy styrene)-graft-hyperbranched Polyglycerol, *ACS Macro Letters,* 2012, 1, 461-1464.

42 G. R. Desiraju, P. S. Ho, L. Kloo, A. C. Legon, R. Marquardt, P. Metrangolo, P. Politzer, G. Resnati, K. Rissanen, Definition of the halogen bond (IUPAC Recommendations 2013), *Pure and Applied Chemistry*, 2013, 85, 1711-1713.

43 A. Sun, J.W Lauher, N. S Goroff, Preparation of poly(diiododiacetylene), an ordered conjugated polymer of carbon and iodine, *Science*, 2006, 312,1030–1034.

44 N. Houbenov, R. Milani, M. Poutanen, J. Haataja, V. Dichiarante, J. Sainio, J. Ruokolainen, G. Resnati, P. Metrangolo, and O. Ikkala, Halogen-bonded mesogens direct polymer self-assemblies up to millimetre length scale, *Nature Communications,* 2014, 5, 4043.

45 W. K. Cameron, K. Pierre, and P. B. Curtis, π covalency in the halogen bond, *Nature Communications,* 2020, 11, 3310.

46 C. J. Paulo, The halogen bond: Nature and applications, Physical Sciences Reviews, 2017, 0136.

47 D. Uhrig and J. W. Mays, Experimental techniques in high-vacuum anionic polymerization, *J. Poly. Sci. Part A: Poly. Chem*., 2005, 43, 6179-6222.

48 N. Hadjichristidis, H. Iatrou, S. Pispas, M. Pitsikalis, Anionic polymerization: High vacuum techniques, *J. Poly. Sci. Part A: Poly. Chem.,* 2000, 38, 3211-3234.

49 L. Junyu, Z. Zhigao, Z. Hui, W. Shanhe, Z. Xiangming, Z. Jianwei, L. Rongliang, D. Quoting, W. Yingsong, L. Guanfeng, Simple and rapid monitoring of doxorubicin using streptavidin-modified microparticle-based time-resolved fluorescence immunoassay, *RSC Adv.,* 2018, 8, 15621-15631.

50 R. H. Still and A. Whitehead, Thermal degradation of polymers. XV. Vacuum pyrolysis studies on poly(p-methoxystyrene) and poly(p-hydroxystyrene), *J. App. Poly. Sci.,* 1977, 21, 1199-1213.

51 Y.-S. Yoo, J.-H. Choi, J.-H. Song, N.-K. Oh, W.-C. Zin, S. Park, T., and Chang, M. Lee, Self-Assembling Molecular Trees Containing Octa-p-phenylene: From Nanocrystals to Nanocapsules, *J. Am. Chem. Soc*., 2004, 126, 6294-6300.

52 S. Zhou , C. Burger, B. Chu , M. Sawamura, N. Nagahama, M. Toganoh, U. E. Hackler, H. Isobe, E. Nakamura, Spherical Bilayer Vesicles of Fullerene-Based Surfactants in Water: A Laser Light Scattering Study, *Scienc*e, 2001 , 291 , 1944-1947.

53 O. M. Adam , K. O. Rachel, Thermally induced micelle to vesicle morphology transition for a charged chain end diblock copolymer, *Chem. Commun.,* 2010, 4 , 1091 – 1093 .

54 G. Cavallo, P. Metrangolo, R. Milani, T. Pilati, A. Priimagi, G. Resnati, and G. Terraneo, The Halogen Bond, *Chemical Reviews*, 2016, 116, 2478-2601.

55 S. Xu and H. Wang, A new entrainer for separation of tetrahydrofuran–water azeotropic mixture by extractive distillation, *Chem. Eng. Process*, 2006, 45, 954-958.

56 J. Facder and B. M. Ladanyi, Molecular Dynamics Simulations of the Interior of Aqueous Reverse Micelles, *Phys. Chem. B,* 2000, 104, 1033-1046.

57 S. Sritharan, N. Sivalingam, A comprehensive review on time-tested anticancer drug doxorubicin, *Life Sci.*, 2021, 278, 119527.

58 H. Taymaz-Nikerel, E. K. Muhammed, E. Serpil, and Betül, K. Doxorubicin induces an extensive transcriptional and metabolic rewiring in yeast cells, *Scientific Reports,* 2018, 8, 13672.